THE JOURNAL OF BIOLOGICAL CHEMISTRY VOL. 284, NO. 47, pp. 32582–32590, November 20, 2009

Myocardin-dependent Activation of the CArG Box-rich Smooth Muscle γ-Actin Gene

*PREFERENTIAL UTILIZATION OF A SINGLE CArG ELEMENT THROUGH FUNCTIONAL ASSOCIATION WITH THE NKX3.1 HOMEODOMAIN PROTEIN**

Received for publication, June 15, 2009, and in revised form, September 14, 2009 Published, JBC Papers in Press, September 21, 2009, DOI 10.1074/jbc.M109.033910

Qiang Sun[‡1], Sebastien Taurin[§], Nan Sethakorn[§], Xiaochun Long[‡], Masaaki Imamura[‡], Da-Zhi Wang[¶2], Warren E. Zimmer[‖3], Nickolai O. Dulin[§4], and Joseph M. Miano[‡5]

From the [‡]Aab Cardiovascular Research Institute of the University of Rochester School of Medicine and Dentistry, Rochester, New York 14642, the [§]Section of Pulmonary and Critical Care, University of Chicago, Chicago, Illinois 60637, the [¶]Department of Cell and Developmental Biology, Carolina Cardiovascular Biology Center, University of North Carolina, Chapel Hill, North Carolina 27599, and the [‖]Systems Biology and Translational Medicine, College of Medicine, Texas A&M Health Science Center, College Station, Texas 77840

Serum response factor (SRF) is a ubiquitously expressed transcription factor that binds a 10-bp element known as the CArG box, located in the proximal regulatory region of hundreds of target genes. SRF activates target genes in a cell- and context-dependent manner by assembling unique combinations of cofactors over CArG elements. One particularly strong SRF cofactor, myocardin (MYOCD), acts as a component of a molecular switch for smooth muscle cell (SMC) differentiation by activating cytoskeletal and contractile genes harboring SRF-binding CArG elements. Here we report that the human *ACTG2* promoter, containing four conserved CArG elements, displays SMC-specific basal activity and is highly induced in the presence of MYOCD. Stable transfection of a non-SMC cell type with *Myocd* elicits elevations in endogenous *Actg2* mRNA. Gel shift and luciferase assays reveal a strong bias for MYOCD-dependent transactivation through CArG2 of the human *ACTG2* promoter. Substitution of CArG2 with other CArGs, including a consensus CArG element, fails to reconstitute full MYOCD-dependent *ACTG2* promoter stimulation. Mutation of an adjacent binding site for NKX3.1 reduces MYOCD-dependent transactivation of the *ACTG2* promoter. Co-immunoprecipitation, glutathione *S*-transferase pulldown, and luciferase assays show a physical and functional association between MYOCD and NKX3.1; no such functional relationship is evident with the related NKX2.5 transcription factor despite its interaction with MYOCD. These results demonstrate the ability of MYOCD to discriminate among several juxtaposed CArG elements, presumably through its novel partnership with NKX3.1, to optimally transactivate the human *ACTG2* promoter.

Smooth muscle cell (SMC)[6] differentiation requires synchronized expression of general and cell-restricted cytoskeletal and contractile genes encoding proteins conferring the unique contractile activity of this cell type (1). Many SMC differentiation genes contain proximal *cis* regulatory elements, called CArG boxes, which bind the broadly expressed transcription factor, serum response factor (SRF) (2). SRF is a weak activator of gene expression, requiring physical interactions among over 60 cofactors that themselves recruit additional proteins to fully direct unique patterns of gene expression. The discovery of one such SRF cofactor, called myocardin (MYOCD), has revolutionized our understanding of the basic transcriptional mechanisms underlying the specification of a differentiated SMC phenotype (3). *Myocd* mRNA is restricted mainly to cardiac and SMC and its encoded protein is one of nature's most powerful transactivators of gene expression (3), although the level of SMC gene activation appears to be both cell and promoter context-dependent (4). MYOCD elicits structural and functional attributes of SMC suggesting this cofactor has characteristics of a master regulator of the differentiated SMC phenotype (5). Consistent with this idea, conventional inactivation of *Myocd* results in midgestational arrest at embryonic day 10.5 of the mouse because dorsal aortic SMC are poorly differentiated (6), a finding that has recently been extended to neural crest-derived SMC of the great arteries (7).

In theory, SRF binds up to 1,216 permutations of the CArG box (8) with the consensus forms (CCW_6GG) binding SRF more avidly than non-consensus forms (9). Many SMC contractile genes contain two or more CArG elements in either their 5′ promoter or intronic regions (2, 10). Olson and colleagues (11) proposed a model wherein MYOCD forms a molecular bridge over two or more CArG boxes by undergoing homo-oligomerization through its leucine zipper-like domain thus maximizing transactivation of SMC contractile genes harboring more than one CArG element. According to this model, SMC cytoskeletal/contractile genes with one CArG box will

* This work was supported, in whole or in part, by National Institutes of Health grants.
[1] Present address: Dept. of Internal Medicine III, University of Heidelberg, Im Neuenheimer Feld 410, 69120 Heidelberg, Germany.
[2] Supported by National Institutes of Health Grants HL075251 and HL085635.
[3] Supported by National Institutes of Health Grants CA095608 and P30 ES09106 to the Center for Environmental and Rural Health, Texas A&M.
[4] Supported by National Institutes of Health Grant HL071755.
[5] Supported by National Institutes of Health Grants HL62572 and HL091168.
To whom correspondence should be addressed: Dept. of Medicine, Box CVRI, University of Rochester School of Medicine and Dentistry, 601 Elmwood Ave., Rochester, NY 14642. Tel.: 585-276-9789; Fax: 585-276-9830; E-mail: j.m.miano@rochester.edu.

[6] The abbreviations used are: SMC, smooth muscle cell; ACTG2, smooth muscle γ-actin; EMSA, electrophoretic mobility shift assay; Myocd, myocardin; NKE, NKX-binding element; RT, reverse transcription; SRF, serum response factor; HA, hemagglutinin; GST, glutathione *S*-transferase.

only be activated moderately by MYOCD. On the other hand, several multi-CArG containing genes are refractory to high level MYOCD-dependent transactivation, which likely is attributable to sequences immediately flanking CArG elements (3, 12–16). Thus, the number of CArG boxes, the sequence character therein, and flanking sequences appear to be key determinants of MYOCD-mediated transcriptional activity.

SMC are often defined structurally and physiologically as vascular or visceral SMC. Although expressing comparable levels of many cytoskeletal/contractile genes, microarray data indicate unique gene expression signatures between both SMC types (17). For example, the SRF- and MYOCD-dependent *telokin* gene is abundantly expressed in visceral SMC with low-level expression in vascular SMC (18). However, a chimeric promoter of *telokin* harboring a fragment of the *Tagln* promoter confers vascular activity in transgenic mice suggesting that SMC promoters harbor important sequence content for vascular *versus* visceral SMC expression (19). Two smoothelin isoforms exhibit SMC type-restricted expression in adults with *smoothelin A* expressed predominantly in visceral SMC and *smoothelin B* in vascular SMC (20). *Smoothelin A* contains conserved CArG elements that are mildly responsive to MYOCD, whereas *smoothelin B*, without conserved CArG boxes, is refractory to MYOCD transactivation *in vitro* (15).

The murine smooth muscle γ-actin gene (*Actg2*) is expressed abundantly in visceral SMC with lower levels in vascular SMC (21). Transgenic mice carrying 13.7 kb of 5′ promoter and 3′ intronic mouse *Actg2* sequences similarly exhibit visceral SMC activity (22). In this report, we have revisited expression of *Actg2* in vascular SMC and evaluated the role of MYOCD in regulating human *ACTG2* promoter activity *in vitro*. Results demonstrate *Actg2* mRNA and protein expression as well as specific promoter activity in vascular SMC. Despite the presence of four closely juxtaposed CArG boxes in the 5′ proximal region of *ACTG2*, MYOCD appears to preferentially utilize a single CArG element (CArG2) that confers high-level promoter activity through elevations in SRF-MYOCD binding. Importantly, an adjacent binding site for NKX3.1 is necessary for full transactivation, and co-transfection reporter assays of MYOCD show NKX3.1 potentiates MYOCD-dependent stimulation of the human *ACTG2* promoter. Co-immunoprecipitation, GST pulldown, and luciferase reporter assays suggest this activity occurs through physical contacts between the C-terminal domain of MYOCD and NKX3.1. These results reveal a CArG bias for MYOCD transactivation of *Actg2* gene transcription and suggest this discrimination stems from the novel interaction of MYOCD with the NKX3.1 homeodomain protein.

EXPERIMENTAL PROCEDURES

Cell Culture—Primary-derived rat aortic smooth muscle cells and the PAC-1 and A7r5 SMC lines, as well as NIH 3T3, CV-1, COS-7, HeLa, BC_3H1, L6 myoblasts, and a human uterine SMC line (SKLMS, ATCC) were maintained in Dulbecco's modified Eagle's medium containing high glucose, supplemented with 10% fetal bovine serum and 200 μM L-glutamine. Cells were cultured in the absence of antibiotics and antimycotics and used for transfections or RNA/protein analysis when 70–90% confluent. The same medium conditions were used for prostate stromal and epithelial cells as well as LNCaP and PC3 prostate cell lines. In some experiments the androgen, methyltrienolone (R1881, PerkinElmer Life Sciences), was used at 1 or 10 nM (see below). For L6 stable cell lines carrying myocardin (4), cells were cultured in the presence of 900 μg/ml G418.

Plasmids—Serial deletions of the human *ACTG2* promoter (285, 205, 95, and 55 nucleotides from the annotated transcriptional start site) were cloned into pGL3 basic (Promega, Madison, WI) for *firefly* luciferase reporter assays (below). Mutations were introduced into each of the four CArG regulatory elements (CArG1, CArG2, CArG3, and CArG4) and NKX-binding element (NKE) of the human *ACTG2* promoter using QuikChange site-directed mutagenesis (Stratagene) and verified by DNA sequencing (Cornell Sequencing Core). The *ACTG2* CArG4 sequence was mutated from the wild type element 5′-gcttataagg-3′ to 5′-*gtc*tataagg-3′, the CArG3 sequence from 5-gcataaaagg-3′ to 5-gtctaaaagg-3′, the CArG2 sequence from 5′-cctatatgg-3′ to 5′-gtctatagg-3′, the CArG1 sequence from 5′-ccttttagg-3′ to 5-gtcttttagg-3′, and the NKE sequence from 5-cgtcagctgg-3′ to 5′-cgtcagcccc-3′. The CArG1, -2, -3, -4, CArG1, -3, -4, and CArG2 mutants contained the same respective mutations as above. Plasmids pcDNA3.1-FLAG-MYOCD and pcDNA3.1-FLAG-MYOCD-ΔCT were used as previously described (3). SRF-VP16, pCGN-HA-NKX2.5, and pCGN-HA-NKX3.1 were used as described (23, 24).

Reverse Transcription-Polymerase Chain Reaction (RT-PCR)—Total RNA was isolated from tissues and cell lines using the TRIzol reagent system (Invitrogen). 4 μg of total RNA was reverse transcribed into cDNA with SuperScript™ III first-strand synthesis (Invitrogen). PCR amplification was then performed with the following primers to the mouse genes of interest: *Gapd*, forward, gccaaaagggtcatcatctc and reverse, ggccatccacagtcttct (226 bp); *Myocd*, forward, cgccaacgacagtgacgaaca and reverse, cgtgaagctcagctgcagac (253 bp); *Srf*, forward, atcaccaactacctggcacc and reverse, cacctgtagctcggtgaggt (594 and 402 bp); *Actg2*, forward, catgaagtgtgacattgacatccgc and reverse, ggcttgaaggttttaatgatctg (356 bp); *Acta2*, forward, accaccatgtacccaggcattgct and reverse, ccacgagtaacaaatcaaagctttgggc (330 bp); *Nkx3.1*, forward, tccttcctcatccaggac and reverse, caggtacttctgatggctg (356 bp); and *Nkx2.5*, forward, cccttctcagtcaaagacatcc, and reverse, gtaccgctgttgcttgaag (451 bp). Adenoviral-mediated short hairpin RNA knockdown of SRF was done in BC_3H1 cells using 25 multiplicity of infection of short hairpin SRF or short hairpin enhanced green fluorescent protein control and levels of the *Actg2* transcript were measured with the above primers. PCR products were resolved in a 1.5% agarose gel and visualized by ethidium bromide staining.

Transient Transfection and Luciferase Assay—The calcium phosphate co-precipitation method was used for transient transfections as described (25). Cells were dispersed in 24-well plates at 50,000 cells/well and grown to subconfluence. Except where indicated, cells were co-transfected with 0.5 μg of *ACTG2* promoter linked to *firefly* luciferase and either 0.5 μg of empty vector (pcDNA3.1 or pCGN) or an equal molar quantity of the same vector carrying various forms of MYOCD, NKX3.1, NKX2.5, or SRF-VP16. Fifty nanograms of the internal *Renilla* reporter gene (Promega) were used in all samples to normalize

luciferase activity. The following day (12–16 h post-transfection), cells were washed with phosphate-buffered saline and refed fresh growth medium for an additional 24 h. Cells were then lysed with 200 μl of 1× Passive lysis buffer (Promega) and 20 μl of cell lysate was processed for Dual Luciferase Assay according to the manufacturer's manual (Promega). Bioluminescence was measured over 10 s with an AutoLumat LB 953 luminometer (EG&G Berthold, Gaithersburg, MD). All transfections were performed in quadruplicate in at least two independent experiments and expressed as the normalized (luciferase to *Renilla*) fold-change over baseline (−55 *ACTG2*, see Fig. 2*B*, and −55 *ACTG2* absent MYOCD in see Fig. 3), percent change under −285 *ACTG2* (see Fig. 5), or fold-increase over pcDNA3.1 or pcGN control vectors (see Fig. 6).

Immunohistochemistry—Sections (5 μm) of rat heart and aorta were processed for immunohistochemistry with an ACTG2-selective antibody as described (26). Under these conditions (>1:500 antibody dilution) we and others have shown that the monoclonal antibody clone B4 used in this study is highly selective for the smooth muscle γ-actin isoform, ACTG2 (48, 49).

Co-immunoprecipitation and Western Blotting—Interactions between NKX3.1 and MYOCD were examined by co-immunoprecipitation following co-transfection with FLAG-tagged MYOCD and HA-tagged NKX3.1. Transfected cells were lysed in immunoprecipitation lysis buffer containing 50 mM Tris-HCl (pH 7.5), 100 mM NaCl, 5 mM $MgCl_2$, 0.5% Nonidet P-40, 1 mM dithiothreitol, 10 mM sodium fluoride, 1 mM sodium orthovanadate, 200 μM phenylmethylsulfonyl fluoride and protease inhibitor mixture (Sigma). Lysates were cleared by centrifugation (5 min at 14,000 rpm), followed by incubation with anti-FLAG antibodies conjugated to agarose beads (M2, Sigma) overnight at 4 °C. The beads were washed three times with lysis buffer, the immune complexes were eluted by boiling in Laemmli buffer for 5 min and subjected to polyacrylamide gel electrophoresis followed by electrotransfer to Immobilon-P membrane (Millipore). The proteins on the membrane were then analyzed by Western blotting with anti-HA or anti-FLAG antibodies followed by horseradish peroxidase-conjugated secondary antibodies (Calbiochem), and developed by enhanced chemiluminescence reagent (Pierce).

In Vitro Binding Assay—The [^{35}S]methionine-labeled *in vitro* translated myocardin probe was generated in rabbit reticulocyte lysate (Promega, Madison, WI), following the manufacturer's protocol. The [^{35}S]MYOCD probe was incubated with purified GST-NKX3.1 or GST alone (bound to glutathione-Sepharose beads) for 3 h at 4 °C in a buffer containing 20 mM HEPES, 75 mM KCl, 1 mM EDTA, 2 mM $MgCl_2$, 0.1% Nonidet P-40, 2 mM dithiothreitol. The resin was subsequently washed four times with 1 ml of the binding buffer, and then boiled in Laemmli sample buffer. Proteins were resolved by SDS-PAGE and transferred to a polyvinylidene difluoride membrane. The proteins on the membrane were stained with Amido Black, and the [^{35}S]MYOCD was detected by autoradiography.

Electrophoretic Mobility Shift Assay (EMSA)—To examine SRF-MYOCD binding to CArG boxes in the human *ACTG2* promoter, the following oligonucleotides (CArG and NKE sites underlined, mutant bases in lowercase) and their respective complement (not shown) were heated at 65 °C for 10 min and annealed prior to end labeling with [γ-^{32}P]dATP as described (27): WT-CArG1, 5′-CACCGTCAGCTGGCCTTTTTAGGGACTTTG-3′; Mut-CArG1, 5′-CACCGTCAGCTGGgtcTTTTAGGGACTTTG3′; WT-CArG2, 5′-GAAAAAACCACCTTATATGGTAATATTGCT-3′; Mut-CArG2, 5′-GAAAAAACCAgtcTATATGGTAATATTGCT-3′; WT-NKE: 5′-GCTAACACACCGTCAGCTGGCCTTTTTAGG-3′; Mut-NKE, 5′-GCTAACACACCGTCAGCcccCCTTTTTAGG-3′.

The wild type *ACTG2* −205 promoter fragment containing CArG1, NKE, and CArG2 was end-labeled using T4 polynucleotide kinase (New England Biolabs). SRF and MYOCD were *in vitro* translated by the TnT Coupled Reticulocyte Lysate system (Promega). Endogenously expressing MYOCD was from lysates of L6 cell lines stably transfected with MYOCD (4). Samples were resolved on a 5% polyacrylamide gel using indicated competitors and antibodies essentially as described (27).

Computational Biology—Comparative sequence analysis of the human *ACTG2* genetic locus with orthologs in chimp (*Pan troglodytes, Ptr*), dog (*Canis familiaris, Cfa*), mouse (*Mus musculus, Mmu*), and chicken (*Gallus gallus, Gga*) was done with the VISTA Gene Alignment tool (28). Sequence logos representing position weight matrices of orthologous CArG and NKE elements of the ACTG2 promoter from the same species as those used in the VISTA analysis were generated with WebLogo (29). Simple protocols for performing these analyses are available upon request.

RESULTS

ACTG2 Expression in Vascular Smooth Muscle and Prostate—*Actg2* mRNA is abundantly expressed in aorta, bladder, and cultured SMC with less expression in other tissues and cell lines (Fig. 1*A*). In contrast, *Acta2* mRNA is more broadly expressed. Interestingly, we observe differential splicing of *Srf* mRNA in aorta and bladder (primarily full-length) *versus* other tissues and cultured SMC (full-length plus δ5 splice variant, Fig. 1*A*); the molecular basis for this differential splicing phenomenon is presently unknown. As expected, *Nkx2.5* mRNA is restricted to heart but detectable transcripts are also seen in the A7r5 SMC line (Fig. 1*A*). Expression of the related *Nkx3.1* mRNA is only seen in L6 myoblasts and A7r5 SMC (the latter cells only show detectable *Nkx3.1* transcripts after two sequential rounds of PCR). *Actg2* and *Nkx3.1* mRNA are present in prostate cell lines (39). To see whether *Myocd* is similarly co-expressed with these transcripts, we measured mRNA levels in several distinct human prostate cell lines in the absence or presence of androgen. Results reveal detectable transcripts to *Myocd* in each cell line (Fig. 1*B*). Moreover, *Myocd* is co-expressed with *Actg2* and *Nkx3.1* mRNA in mouse prostate tissue (Fig. 1*C*). To determine whether expression of the ACTG2 protein coincides with its mRNA expression in vascular SMC, we performed immunohistochemistry with an ACTG2-selective antibody on sections of rat heart and aorta. Levels of ACTG2 protein are present in coronary artery, aortic and microvascular SMC (Fig. 1*D*, *d*, *e*, and *f*, respectively), but not cardiomyocytes (Fig. 1*D*, *d*) or perivascular tissue (Fig. 1*D*, *f*). Together, the expression data establish mRNA and protein expression of SM γ-actin (*Actg2*)

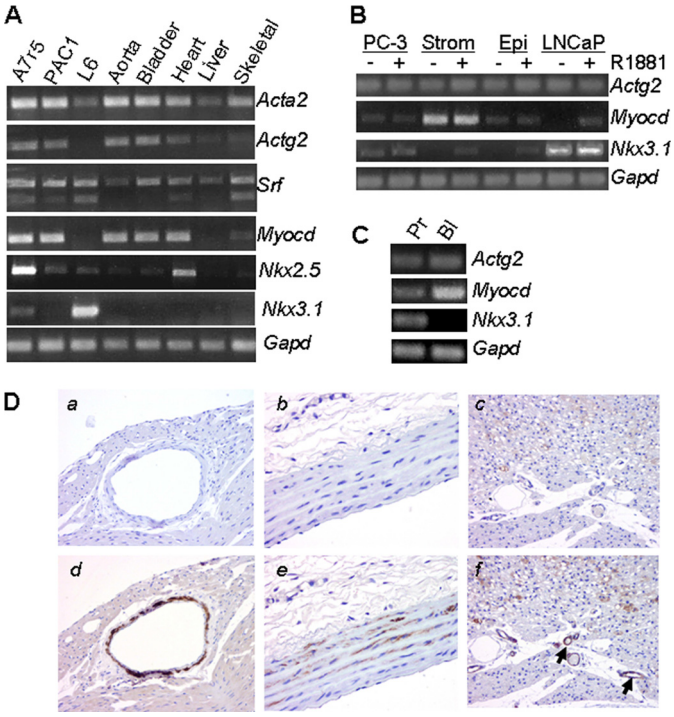

FIGURE 1. **ACTG2 expression in cell lines and tissues.** *A*, RT-PCR analysis showing mRNA expression of SMC γ-actin (*Actg2*) and other SMC markers and transcription factors in various tissues and cell culture models. Note the widespread expression of full-length (*upper band*) *Srf* but restricted expression of the δ5 splice variant (*lower band*) of *Srf* (47) to cultured cells and skeletal muscle and heart, but not aortic medial SMC. *B*, RT-PCR analysis of the indicated markers in various prostate cell lines treated with either 1 (Strom and Epi) or 10 nM (PC-3 and LNCaP) androgen (R1881). Abbreviations used are prostate stromal cells, *Strom;* and prostate epithelial cells, *Epi*. *C*, RT-PCR analysis of the indicated markers in prostate (*Pr*) and bladder (*Bl*). *D*, ACTG2 protein expression (*brown*) in coronary artery (*d*), aorta (*e*), and microvessels of rat perivascular tissue (*arrows* in *f*). Specificity of staining is indicated by the absence of signal when using an isotype-matched IgG control antibody (*panels a–c*). Magnifications are ×200.

in distinct vascular SMC types and the co-expression of *Myocd*, *Nkx3.1*, and *Actg2* mRNA in prostate tissue/cell lines.

SMC-specific Basal and MYOCD-dependent Activation of Actg2—Comparative genomics between human (Hsa) and chimp (Ptr), dog (Cfa), mouse (Mmu), and chicken (Gga) reveals high sequence conservation in the immediate 5′ promoter region of *ACTG2* where 4 conserved CArG elements and a binding element for NK factors (NKE) reside over ~200 bp of genomic DNA (Fig. 2, *A* and *B*). The presence of CArG1 and NKE elements mediates mild basal promoter activity in several SMC lines from human and rat (−*95* in Fig. 2*C*). Inclusion of CArG2 dramatically elevates basal human *ACTG2* promoter activity in a SMC-specific manner (−*205* in Fig. 2*C*). The addition of CArG3 and CArG4 has no further stimulatory effect on *ACTG2* promoter activity in SMC (−285 in Fig. 2*C*). To determine the relative effects of MYOCD on each *ACTG2* promoter construct, transient co-transfections were performed in COS7 and the rat pulmonary artery PAC1 SMC line using the 807-amino acid form of MYOCD (3) (Fig. 3, *A* and *B*). In both COS7 and PAC1 SMC, MYOCD is unable to stimulate increases in the *ACTG2* −55 promoter construct above baseline levels and only mildly stimulates −95 *ACTG2*. However, addition of CArG2 (−205) results in 100-fold increases in *ACTG2* promoter activity in COS7 cells (Fig. 3*A*). Less apparent induction is seen with −205 *ACTG2* in PAC1 SMC due to the higher basal activity of the −205 reporter (Fig. 3*B*). Similar to data in Fig. 2*C*, the presence of CArG3 and CArG4 (−285) confers no further MYOCD-dependent transactivation of *ACTG2* promoter activity (Fig. 3, *A* and *B*). Consistent with previous data using other CArG-dependent promoters (3), the basic and C-terminal transactivation domain of MYOCD are essential in mediating *ACTG2* promoter stimulation (data not shown). To determine whether the potent stimulation of MYOCD on the *ACTG2* promoter translates into activation of the endogenous rat *Actg2* gene, we evaluated mRNA expression levels of *Actg2* in L6 myoblasts stably transfected with *Myocd*. In three independent stable cell lines, the presence of *Myocd* transcripts correlated with induction of the *Actg2* mRNA (Fig. 3*C*). Moreover, RNA knockdown of SRF in BC_3H1 cells elicits corresponding decreases in endogenous *Actg2* transcripts (Fig. 3*D*). Together, these results firmly establish *Actg2* as an SRF-MYOCD-dependent SMC target gene, consistent with previous expression studies (11).

SRF-Myocardin Preferentially Binds CArG2 of the Human ACTG2 Promoter—A previous study using the chicken *Actg2* promoter showed differential binding of SRF to each of the 4 conserved CArG elements (26). We used EMSA to assess the association of MYOCD with SRF bound to CArG1 or CArG2 of the human *ACTG2* −205 promoter because luciferase data reveal high level activity within this region (Fig. 3, *A* and *B*). A nucleoprotein ternary complex of *in vitro* translated SRF and MYOCD can readily be seen and validated with appropriate antibodies to SRF and FLAG-tagged MYOCD (Fig. 4, *lanes 5–7*). Competitive EMSA experiments with cold −205 probe or CArG2 oligonucleotide disrupt CArG-SRF-MYOCD ternary complex formation, whereas CArG1 or NKE have minimal effect (Fig. 4, *lanes 8–11*). These results suggest that SRF-MYOCD associate preferentially with CArG2 of the human *ACTG2* −205 promoter.

We next evaluated effects of point mutations in each of the 4 CArG elements or NKE on the ability of MYOCD to transactivate the *ACTG2* promoter. Mutations in CArG1, -3, and -4, leaving CArG2 intact, mildly reduce MYOCD transactivation of the *ACTG2* −285 promoter (Fig. 5*A*). On the other hand, mutating CArG2 in context of wild type CArG1, -3, and -4 completely abolishes MYOCD-dependent transactivation of the *ACTG2* promoter suggesting that CArG2 is the preferred CArG element MYOCD utilizes for *ACTG2* transcription (Fig. 5*A*). Surprisingly, mutation of NKE (without CArG mutations) also reduces MYOCD-dependent transactivation suggesting that NKE and one of its binding proteins may influence the ability of MYOCD to activate through CArG2 (see below). Similar results are seen in other cell types (L6 and HeLa) and with the *ACTG2* −205 promoter (data not shown).

We next performed EMSA with the *ACTG2* −285 promoter (with 4 CArG boxes) as a probe; chromatin immunoprecipitations cannot adequately discriminate SRF-MYOCD association between such closely juxtaposed CArG elements. We find that mutation of all 4 CArGs is incompatible with SRF-MYOCD ternary complex formation (Fig. 5*B*, *lane 2 versus lane 1*). Consistent with the luciferase activity above, the same probe with only CArG2 intact supports full binding activity (*lane 3 versus lane 1*), but mutation of CArG2 in the context of WT CArG1/

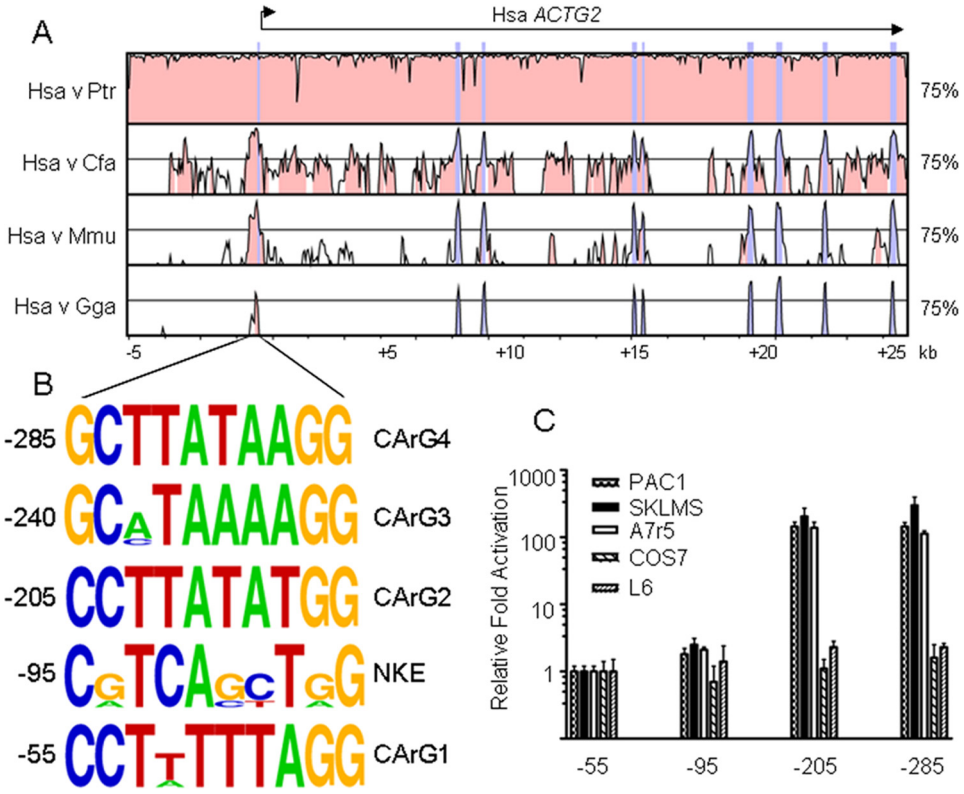

FIGURE 2. **Basal *ACTG2* promoter activity.** *A*, VISTA plot of the 9-exon human (*Hsa*) *ACTG2* gene (denoted at the *top* with the *bent arrow* indicating the transcription start site) *versus* orthologs in chimp (*Ptr*), dog (*Cfa*), mouse (*Mmu*), and chicken (*Gga*). *Blue vertical peaks* indicate exons, whereas *pink peaks* indicate at least 75% sequence homology over 100 bp of non-coding sequence. Note the progressive loss in non-coding sequence homology from chimp to chicken. *B*, sequence logos for the 5 major *cis*-acting elements in the immediate 5′ promoter region of *ACTG2*. These logos represent position weight matrices derived from human, chimp, dog, mouse, and chicken orthologous sequence elements (position of human elements relative to transcription start site indicated at the *left* of each logo). Note that CArG4 and CArG2 are 100% homologous across all species analyzed. Where sequences diverge in other elements, the *height of the letters* diminishes with inclusion of variant base sequences. *C*, firefly luciferase activities of various human *ACTG2* promoter constructs in 3 distinct SMC lines (PAC1 pulmonary artery, human SKLMS uterine SMC, and A7r5 aortic SMC) *versus* two non-SMC types (COS7 and L6). Luciferase activity is presented here as the fold-activation of normalized (ratio of luciferase to *Renilla* control) luciferase to the minimal −55 promoter, set to 1. Each *bar* represents the average (and standard deviation) of 4 replicates in each of the indicated cells lines. These experiments were performed multiple times with similar trends in relative fold-activation. Note the *y* axis here and in Fig. 3 is based on a logarithmic scale.

3/4 leads to near complete loss in SRF-MYOCD ternary complex formation (*lane 4*). Competitive EMSA studies further substantiate the pivotal role of CArG2 in SRF-MYOCD binding to the *ACTG2* −285 promoter (*lanes 6–11*). We next determined the effects of substituting CArG2 with other CArG elements on *ACTG2* promoter activity and SRF-MYOCD complex formation. Substantial loss in both promoter activity (Fig. 5*C*) and SRF-MYOCD ternary complex formation (Fig. 5*B*, *lanes 12–15*) is seen when CArG2 is replaced with any of the other CArG elements of the *ACTG2* promoter. Taken together, results support the concept of MYOCD preferentially utilizing a single CArG element (CArG2), among many, to effect *ACTG2* gene transcription.

NXK3.1 Potentiates ACTG2 Promoter Activity and Physically Associates with MYOCD—Because mutation of the NKE site adjacent to CArG1 reduces MYOCD-dependent transactivation of the *ACTG2* promoter (Fig. 5*A*), we hypothesized that NKX3.1 would augment MYOCD-dependent *ACTG2* promoter activity. Initial co-transfection studies with NKX3.1 and MYOCD failed to show any additive effect of NKX3.1 on *ACTG2* promoter activity, probably because the level of MYOCD expression was high thus masking any positive effect of NKX3.1 (data not shown). However, when we reduce the concentration of MYOCD >10-fold, a strong stimulatory effect of NKX3.1 is observed in COS7 cells (Fig. 6*A*). This effect requires MYOCD and is specific for NKX3.1 as the related NKX2.5 factor is without effect (Fig. 6*A*) despite its apparently higher expression (Fig. 7*A*, *lower panel*). The effect of NKX3.1 on MYOCD-dependent transactivation is dose-dependent (Fig. 6*B*) and specific for the *ACTG2* promoter as no such activity is seen with other SMC promoters or the *ACTG2* −95 promoter (data not shown). Moreover, similar findings are seen in HeLa and L6 cells indicating the effects are not restricted to only one cell type (data not shown). Similar to data in Fig. 5*A*, the synergistic stimulation for NKX3.1 of the *ACTG2* promoter activity is severely attenuated when either CArG2 or the NKE site is mutated (Fig. 6*C*). Collectively, these results suggest MYOCD functionally associates with NKX3.1 to effect *ACTG2* transcription.

To ascertain whether the functional association between NKX3.1 and MYOCD extends to a physical interaction, we performed co-immunoprecipitations in COS7 cells co-transfected with *Myocd* and *Nkx3.1* or *Nkx2.5*. Both NKX factors interact with MYOCD (Fig. 7*A*, *middle panel*) and the interaction of NKX3.1 was lost when the C-terminal transactivation domain of MYOCD was deleted (Fig. 7*B*, *middle panel*). The direct interaction between MYOCD and NKX3.1 was confirmed by the *in vitro* binding assay of [^{35}S]MYOCD with GST-NKX3.1 (Fig. 7*C*). These results strongly suggest that NKX3.1 mediates its MYOCD-dependent transactivation of *ACTG2* transcription via direct physical contact through the C-terminal transactivation domain of MYOCD.

DISCUSSION

The results of this report demonstrate expression of SM γ-actin (ACTG2) in vascular SMC *in vitro* and *in vivo*, thereby validating this traditionally viewed visceral SMC marker (26), a vascular SMC marker as well. The human *ACTG2* promoter, containing four conserved CArG elements, exhibits SMC-specific promoter activity *in vitro* and is highly responsive to MYOCD-dependent transactivation. Several lines of evidence support MYOCD preferentially utilizing a single CArG element

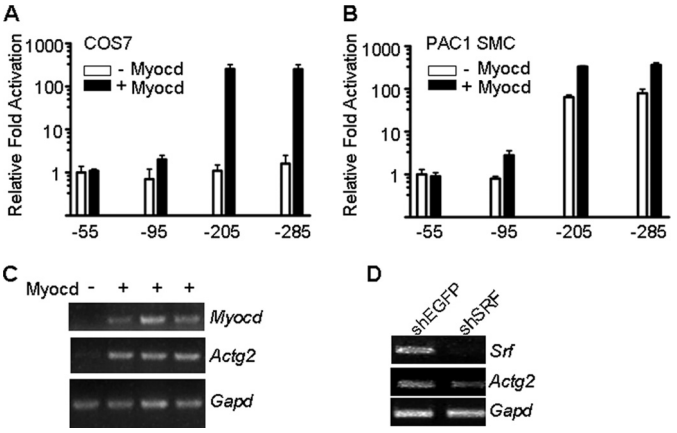

FIGURE 3. **MYOCD-dependent stimulation of *ACTG2* promoter and endogenous mRNA.** COS7 (*A*) or PAC1 SMC (*B*) were co-transfected with the indicated human *ACTG2* promoters linked to luciferase in the absence (*open bars*) or presence (*closed bars*) of MYOCD and resulting activities determined as described in the legend to Fig. 1. Similar results were found in two independent experiments. *C*, semi-quantitative RT-PCR analysis shows endogenous *Actg2* mRNA induction in three independent L6 myoblast clones stably transfected with *Myocd*, but not in similarly grown L6 cells carrying an empty expression vector. A housekeeping gene (*Gapd*) serves as a loading control. *D*, knockdown of SRF in BC_3H1 cells reveals decreases in *Actg2* mRNA expression. *shEGFP*, short hairpin enhanced green fluorescent protein (shEGFP).

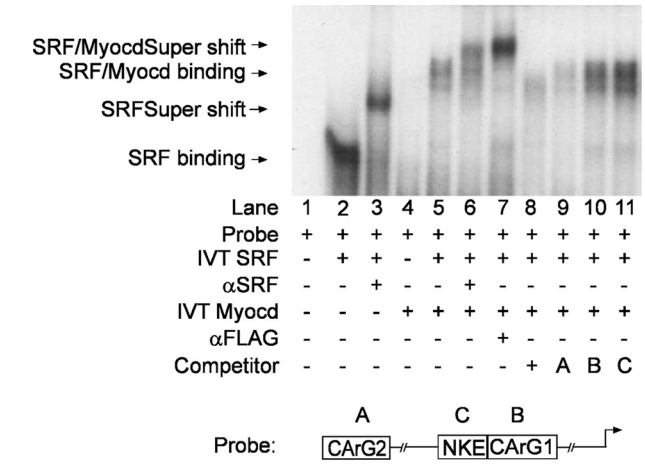

FIGURE 4. **SRF-MYOCD ternary complex formation on the *ACTG2* promoter.** EMSA showing SRF/FLAG-MYOCD binding to a radiolabeled *ACTG2* −205 probe containing CArG2, CArG1, and NKE (labeled *A*, *B*, and *C*, respectively, in the schematic at the *bottom*). The probe supports SRF binding (*lane 2*), which is supershifted with an antibody to SRF (*lane 3*), but not MYOCD binding alone (*lane 4*). A ternary complex is seen when SRF and MYOCD are combined (*lane 5*) and this complex is supershifted with antibodies to SRF (*lane 6*) or FLAG (*lane 7*). Ternary complex is competed with the cold −205 probe (*lane 8*) or CArG2 (*lane 9*), but not CArG1 (*lane 10*) or NKE (*lane 11*) oligonucleotides. Similar results are seen when using whole cell lysates of L6 myoblasts stably transfected with FLAG-MYOCD as the source of MYOCD (data not shown).

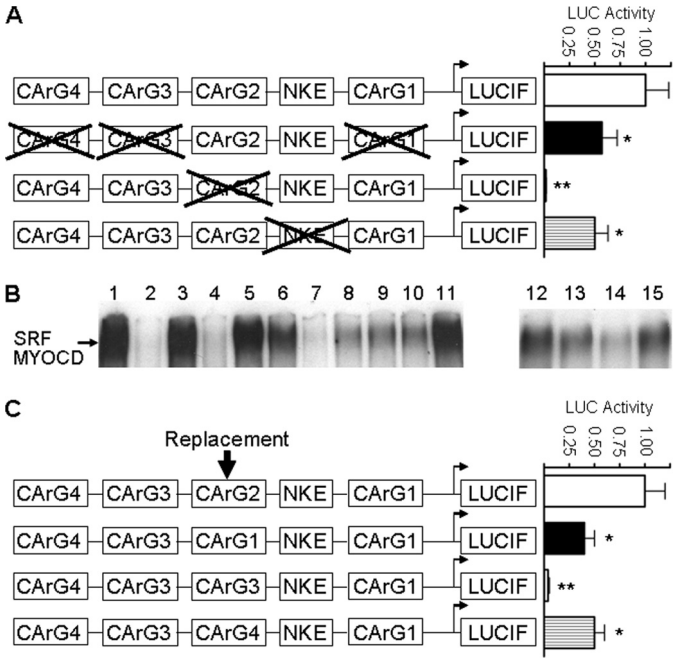

FIGURE 5. **ACTG2 CArG2 is the major determinant for SRF-MYOCD binding and activity.** *A*, luciferase activities (normalized fold-change *versus* wild type *ACTG2* −285 set to 1) in COS7 cells co-transfected with the indicated mutant promoters and MYOCD. Each *bar* represents the average (and S.D.) of 4 replicates and is representative of several independent experiments. *B*, EMSA of *in vitro* translated SRF and MYOCD with wild type and various mutants of the *ACTG2* −285 promoter, used as radiolabeled probes. Presence or absence of nucleoprotein complexes with wild type (*lanes 1* and *6*), mutant CArG1–4 (*lane 2*), mutant CArG1, -3, and -4 (*lane 3*), mutant CArG2 (*lane 4*), or mutant NKE (*lane 5*) probes. Variable reductions in SRF-MYOCD nucleoprotein complexes with the −285 *ACTG2* probe are seen with ×100 cold competitor oligonucleotides to CArG2 (*lane 7*), CArG1 (*lane 8*), CArG3 (*lane 9*), CArG4 (*lane 10*), and NKE (*lane 11*). SRF-MYOCD complexes with wild type −285 *ACTG2* probe (*lane 12*) and the same probe with CArG substitutions as follows: CArG2 > CArG1 (*lane 13*), CArG2 > CArG3 (*lane 14*), or CArG2 > CArG4 (*lane 15*). *C*, luciferase activities (as in *panel A*) following MYOCD-dependent activation of the indicated *ACTG2* −285 promoter constructs in COS7 cells. *Single* and *double asterisks* indicate statistical significance at 0.05 and 0.01, respectively.

for transactivation of *ACTG2*. First, we show through mutagenesis studies that MYOCD mediates *ACTG2* transcription primarily through CArG2. Second, the CArG2 sequence is shown to confer the highest level of SRF-MYOCD binding. Finally, replacing CArG2 with another consensus CArG (CArG1) only weakly activates the *ACTG2* promoter demonstrating that the sequence character of CArG2 is critical for MYOCD-dependent transactivation. Mutation of a binding site for NKX3.1 (24), adjacent to CArG2, reduces MYOCD-dependent transactivation of *ACTG2*, suggesting a functional association between NKX3.1 and MYOCD. Indeed, we show that NKX3.1 potentiates the activity of MYOCD in a CArG2- and NKE-dependent manner, and binding assays reveal direct association of NKX3.1 to the C-terminal domain of MYOCD. Taken in aggregate, the results suggest a novel mechanism for the ability of MYOCD to discriminate among multiple CArG boxes through the physical and functional association of MYOCD with the NKX3.1 homeodomain protein.

In mammals, there are six major actin isoforms encoded by separate genes that are transcribed as six independent transcripts encoding proteins with >90% amino acid identity (30). All six actin genes contain at least one SRF-binding CArG element that is important for gene transcription (8), yet each gene displays unique expression patterns during development and in postnatal tissues (21, 31). The manner in which the ubiquitous SRF transcription factor mediates such disparate patterns of gene expression relates to its ability to recruit and bind context- or cell-restricted transcription factors, some of which associate with neighboring *cis* elements. For example, the cardiac α-actin (*Actc1*) promoter has CArG elements that bind SRF and NKX2.5, both of which counter the repressive effects of another CArG-binding factor, YY1 (32). SRF and NKX2.5 physically

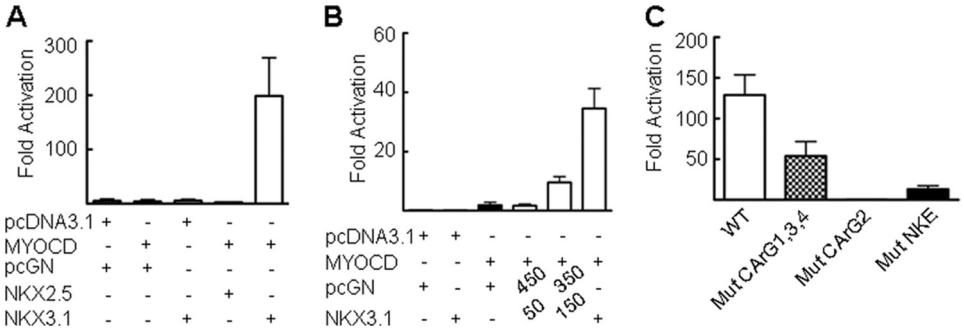

FIGURE 6. **NKX3.1 potentiates MYOCD-dependent activation of the *ACTG2* promoter.** *A*, COS7 cells were co-transfected with the *ACTG2* −285 promoter plus the indicated plasmids, and luciferase activity (per "Experimental Procedures") was measured 24 h later. The amount of MYOCD input was 50 ng, whereas NK factors were used at 500 ng. Results are displayed as the mean ± S.D. and are representative of two independent studies. *B*, similar study as in *panel A* only the amount of NKX3.1 input was varied and balanced by the empty pcGN vector control. *C*, the wild type *ACTG2* −285 promoter or the indicated mutants were co-transfected with 50 ng of MYOCD and 500 ng of NKX3.1 and luciferase activity measured (per "Experimental Procedures"). Results are displayed as those in *panels A* and *B*.

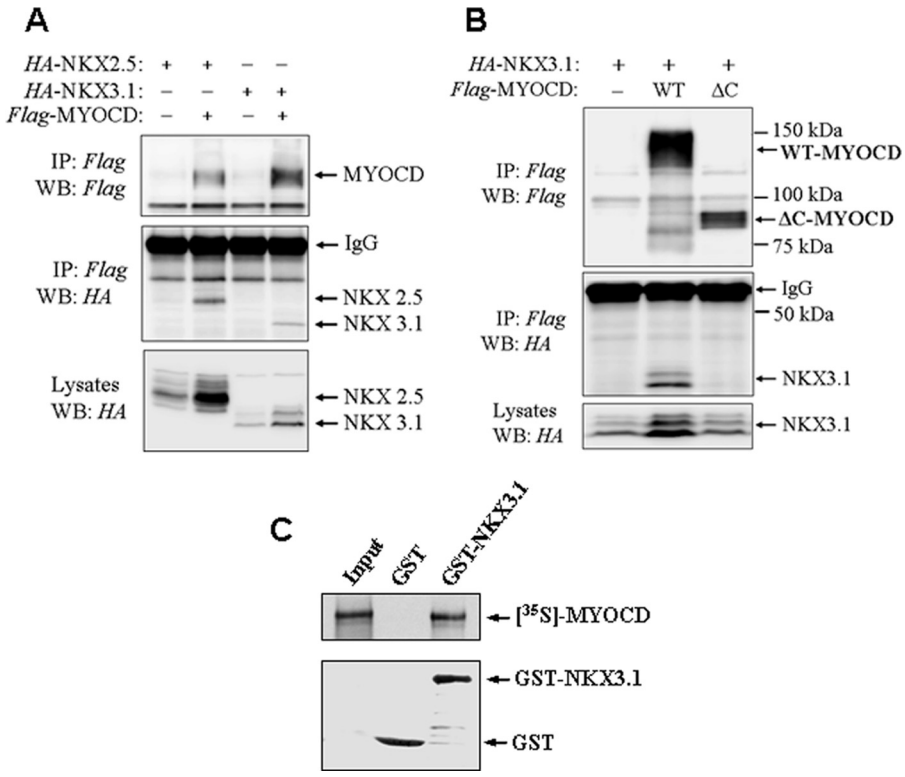

FIGURE 7. **Interaction of myocardin with NKX3.1 and NKX2.5.** *A* and *B*, COS7 cells were transfected with cDNAs for FLAG-tagged full-length myocardin (*WT*) or its truncated mutant with deleted C-terminal transactivation domain (Δ*C*) together with HA-tagged NKX3.1 or NKX2.5. Cells were lysed and the cleared cell extracts were subjected to immunoprecipitation (*IP*) with FLAG antibodies followed by Western blotting (*WB*) of immune complexes (*IP*) or total cell lysates with FLAG or HA antibodies. *C*, *in vitro* binding of [^{35}S]MYOCD with GST-Nkx3.1.

associate and the latter is proposed to direct expression of *Actc1* independent of its ability to bind DNA (33, 34). Thus, vertebrate hearts express the cardiac isoform of actin largely through the coordinate activities of SRF and heart-restricted factors such as NKX2.5. The notable lack of NKX3.1 expression in heart (35–37) could explain, in part, the weak expression of *Actg2* in the myocardium (36) (and Fig. 1) despite the presence of MYOCD. These examples highlight a broader complex regulation of SRF-dependent muscle-restricted genes through the coordinate activities of over 60 SRF cofactors (8).

Previously we showed that a proximal CArG box of the chicken *Actg2* promoter binds SRF avidly through an interaction with NKX3.1 that binds an NKE adjacent to the CArG box (24). In this report, we further advance this concept by showing a functional and physical interaction between NKX3.1 and MYOCD. The functional association of NKX3.1 with MYOCD appears to be unique because a related homeodomain protein (NKX2.5) binds MYOCD but shows no activity over the *ACTG2* promoter. It is possible that interactions between MYCOD and NKX2.5 potentiate cardiac-restricted genes.

Currently available assays could not reveal the presence of a complex between SRF, MYOCD, and NKX3.1 (not shown); however, we postulate that a multiprotein complex encompassing these and perhaps other factors over CArG2 and NKE exists to optimally transactivate the *ACTG2* promoter in a context-dependent fashion. One such context may be the prostate epithelium where levels of *Nkx3.1* (35, 37–39), *Actg2* (40), and possibly *Myocd* (this report) are expressed. Loss in NKX3.1 results in defects of the prostate, including hyperplasia of the ductal epithelium with no obvious defects in vascular tissues (38, 39). Whether levels of ACTG2 are reduced in the prostate or vascular tissues from *Nkx3.1* null mice is currently unknown. Interestingly, ACTG2 and NKX3.1 are considered tumor suppressors with the former part of a molecular signature for human metastatic disease (41). MYOCD is also known to reduce growth (4) and itself has been implicated as a tumor suppressor (42). Thus, it may be important to maintain normal levels of NKX3.1, ACTG2, and MYOCD for normal prostate function.

Although there are four closely spaced CArG boxes within the *ACTG2* promoter, the two proximal sequences, CArG1 and CArG2, are the most avid players with regard to MYOCD-mediated transcriptional responses. This would be consistent with the concept advanced by Olson and colleagues (11) that proposes MYOCD acting as a molecular bridge between adjacent CArG boxes in CArG-rich promoters to mediate strong, cell-specific transcription (43). However, there are exceptions to the

multi-CArG, MYOCD responsive target gene concept including *Egr1* and *Akap12α* promoters, which contain multiple CArG elements but are nevertheless refractory to MYOCD-dependent transactivation (12, 14) (data not shown). Additionally, there are single CArG-containing gene promoters, such as *telokin* and *Cald1*, that are strongly activated by MYOCD (16, 44). Although the bulk of evidence supports the concept of MYOCD-dependent gene activation requiring multiple CArG sequences, the growing exceptions to this idea may indicate a role for accessory proteins to potentiate or modify cell-specific MYOCD-mediated responses. In the activation of *Egr1* transcription, there appears to be a competitive inhibition of MYOCD response by association of ELK1 with SRF (13). As indicated in our studies, MYOCD-mediated transcription of *ACTG2* is potentiated by its interaction with the homeodomain, NKX3.1. The functional consequences of this interaction are dependent upon DNA context as shown by the inability of NKX2.5-MYOCD complexes to activate *ACTG2* promoters. Thus our results support the concept that MYOCD-mediated transcriptional responses require CArG context within the promoter/activator segment as well as the appropriate association of multiple proteins within the transcriptional complex.

Two of the four CArG elements in the *ACTG2* promoter (CArG3 and CArG4) are non-consensus CArG boxes that bind SRF weakly (26) and confer no further MYOCD-dependent transactivation. Therefore, the *ACTG2* promoter presents a model to gain an understanding of MYOCD-modulated, cell-specific transcriptional activation in promoters containing active and inactive CArG elements. Similar to *ACTG2*, the *TAGLN* promoter contains two similarly spaced CArG boxes within its 5′ proximal promoter. Although this gene is highly MYOCD inducible, studies in transgenic mice have shown that a single CArG box is responsible for cell-specific promoter activity (45, 46), indicating that multiple CArGs may participate in gene activation through several mechanisms. Thus, it is possible that the *ACTG2* non-consensus CArG boxes play an important context-dependent role in appropriate MYOCD/SRF transcriptional responses. Of note is our previous studies demonstrating a time- dependent binding of SRF to CArG3 and CArG4 in SMC with elevated SRF expression (26). This would indicate that promoter context plays a significant role in appropriate cell-specific transcription. That is, these distal elements may potentiate *ACTG2* transcription that was initiated by MYOCD-dependent activation at the proximal CArG elements resulting in appropriate SMC *ACTG2* expression. Alternatively, there may be little functionality of these sequences and their conservation may simply reflect their juxtaposition to a block of sequence resistant to genetic drift. It will be important to address these questions in transgenic mice where each of the *ACTG2* CArG elements is mutated.

In summary, we provide new insight into the transcriptional regulation of a CArG-rich human SMC-restricted promoter, *ACTG2*. The finding that SRF and MYOCD utilize a distinct CArG element, even among a cluster of similar elements over a short genomic landscape, supports a model wherein the sequence content of the CArG box, *per se*, imparts structural information that dictates how SRF-associated factors such as MYOCD interact. Molecular structure studies of different SRF-CArG nucleoproteins in the absence or presence of MYOCD will likely offer novel insight into how the CArG sequence character confers MYOCD-dependent transactivation.

Acknowledgment—We thank Mary Georger for performing the immunohistochemistry.

REFERENCES

1. Owens, G. K., Kumar, M. S., and Wamhoff, B. R. (2004) *Physiol. Rev.* **84,** 767–801
2. Miano, J. M. (2003) *J. Mol. Cell. Cardiol.* **35,** 577–593
3. Wang, D., Chang, P. S., Wang, Z., Sutherland, L., Richardson, J. A., Small, E., Krieg, P. A., and Olson, E. N. (2001) *Cell* **105,** 851–862
4. Chen, J., Kitchen, C. M., Streb, J. W., and Miano, J. M. (2002) *J. Mol. Cell. Cardiol.* **34,** 1345–1356
5. Long, X., Bell, R. D., Gerthoffer, W. T., Zlokovic, B. V., and Miano, J. M. (2008) *Arterioscler. Thromb. Vasc. Biol.* **28,** 1505–1510
6. Li, S., Wang, D. Z., Wang, Z., Richardson, J. A., and Olson, E. N. (2003) *Proc. Natl. Acad. Sci. U.S.A.* **100,** 9366–9370
7. Huang, J., Cheng, L., Li, J., Chen, M., Zhou, D., Lu, M. M., Proweller, A., Epstein, J. A., and Parmacek, M. S. (2008) *J. Clin. Invest.* **118,** 515–525
8. Miano, J. M., Long, X., and Fujiwara, K. (2007) *Am. J. Physiol. Cell Physiol.* **292,** C70–C81
9. Leung, S., and Miyamoto, N. G. (1989) *Nucleic Acids Res.* **17,** 1177–1195
10. Reecy, J. M., Belaguli, N. S., and Schwartz, R. J. (1999) in *Heart Development* (Harvey, R. P., and Rosenthal, N., eds) pp. 273–290, Academic Press, New York
11. Wang, Z., Wang, D. Z., Pipes, G. C., and Olson, E. N. (2003) *Proc. Natl. Acad. Sci. U.S.A.* **100,** 7129–7134
12. Cen, B., Selvaraj, A., Burgess, R. C., Hitzler, J. K., Ma, Z., Morris, S. W., and Prywes, R. (2003) *Mol. Cell. Biol.* **23,** 6597–6608
13. Wang, Z., Wang, D. Z., Hockemeyer, D., McAnally, J., Nordheim, A., and Olson, E. N. (2004) *Nature* **428,** 185–189
14. Streb, J. W., and Miano, J. M. (2005) *J. Biol. Chem.* **280,** 4125–4134
15. Rensen, S. S., Niessen, P. M., Long, X., Doevendans, P. A., Miano, J. M., and van Eys, G. J. (2006) *Cardiovasc. Res.* **70,** 136–145
16. Zhou, J., and Herring, B. P. (2005) *J. Biol. Chem.* **280,** 10861–10869
17. Chi, J. T., Rodriguez, E. H., Wang, Z., Nuyten, D. S., Mukherjee, S., van de Rijn, M., van de Vijver, M. J., Hastie, T., and Brown, P. O. (2007) *PLoS Genet.* **3,** 1770–1784
18. Gallagher, P. J., and Herring, B. P. (1991) *J. Biol. Chem.* **266,** 23945–23952
19. Hoggatt, A. M., Simon, G. M., and Herring, B. P. (2002) *Circ. Res.* **91,** 1151–1159
20. van Eys, G. J., Niessen, P. M., and Rensen, S. S. (2007) *Trends Cardiovasc. Med.* **17,** 26–30
21. McHugh, K. M., Crawford, K., and Lessard, J. L. (1991) *Dev. Biol.* **148,** 442–458
22. Qian, J., Kumar, A., Szucsik, J. C., and Lessard, J. L. (1996) *Dev. Dyn.* **207,** 135–144
23. Sun, Q., Chen, G., Streb, J. W., Long, X., Yang, Y., Stoeckert, C. J., Jr., and Miano, J. M. (2006) *Genome Res.* **16,** 197–207
24. Carson, J. A., Fillmore, R. A., Schwartz, R. J., and Zimmer, W. E. (2000) *J. Biol. Chem.* **275,** 39061–39072
25. Graham, F. L., and van der Eb, A. J. (1973) *Virology* **52,** 456–467
26. Browning, C. L., Culberson, D. E., Aragon, I. V., Fillmore, R. A., Croissant, J. D., Schwartz, R. J., and Zimmer, W. E. (1998) *Dev. Biol.* **194,** 18–37
27. Miano, J. M., Carlson, M. J., Spencer, J. A., and Misra, R. P. (2000) *J. Biol. Chem.* **275,** 9814–9822
28. Mayor, C., Brudno, M., Schwartz, J. R., Poliakov, A., Rubin, E. M., Frazer, K. A., Pachter, L. S., and Dubchak, I. (2000) *Bioinformatics* **16,** 1046–1047
29. Crooks, G. E., Hon, G., Chandonia, J. M., and Brenner, S. E. (2004) *Genome Res.* **14,** 1188–1190
30. Vandekerckhove, J., and Weber, K. (1978) *J. Mol. Biol.* **126,** 783–802
31. Schwartz, R. J., and Rothblum, K. N. (1981) *Biochemistry* **20,** 4122–4129
32. Chen, C. Y., and Schwartz, R. J. (1997) *Mol. Endocrinol.* **11,** 812–822

33. Chen, C. Y., and Schwartz, R. J. (1996) *Mol. Cell. Biol.* **16,** 6372–6384
34. Chen, C. Y., Croissant, J., Majesky, M., Topouzis, S., McQuinn, T., Frankovsky, M. J., and Schwartz, R. J. (1996) *Dev. Genet.* **19,** 119–130
35. Bieberich, C. J., Fujita, K., He, W. W., and Jay, G. (1996) *J. Biol. Chem.* **271,** 31779–31782
36. Tanaka, M., Kasahara, H., Bartunkova, S., Schinke, M., Komuro, I., Inagaki, H., Lee, Y., Lyons, G. E., and Izumo, S. (1998) *Dev. Genet.* **22,** 239–249
37. Stanfel, M. N., Moses, K. A., Carson, J. A., Zimmer, D. B., DeMayo, F., Schwartz, R. J., and Zimmer, W. E. (2006) *Genesis* **44,** 550–555
38. Bhatia-Gaur, R., Donjacour, A. A., Sciavolino, P. J., Kim, M., Desai, N., Young, P., Norton, C. R., Gridley, T., Cardiff, R. D., Cunha, G. R., Abate-Shen, C., and Shen, M. M. (1999) *Genes Dev.* **13,** 966–977
39. Schneider, A., Brand, T., Zweigerdt, R., and Arnold, H. H. (2000) *Mech. Dev.* **95,** 163–174
40. Filmore, R. A., Dean, D. A., and Zimmer, W. E. (2002) *Gene Expr.* **10,** 201–211
41. Ramaswamy, S., Ross, K. N., Lander, E. S., and Golub, T. R. (2003) *Nat. Genet.* **33,** 49–54
42. Milyavsky, M., Shats, I., Cholostoy, A., Brosh, R., Buganim, Y., Weisz, L., Kogan, I., Cohen, M., Shatz, M., Madar, S., Kalo, E., Goldfinger, N., Yuan, J., Ron, S., MacKenzie, K., Eden, A., and Rotter, V. (2007) *Cancer Cell* **11,** 133–146
43. Pipes, G. C., Sinha, S., Qi, X., Zhu, C. H., Gallardo, T. D., Shelton, J., Creemers, E. E., Sutherland, L., Richardson, J. A., Garry, D. J., Wright, W. E., Owens, G. K., and Olson, E. N. (2005) *Dev. Biol.* **288,** 502–513
44. Hayashi, K., Nakamura, S., Nishida, W., and Sobue, K. (2006) *Mol. Cell. Biol.* **26,** 9456–9470
45. Li, L., Liu, Z., Mercer, B., Overbeek, P., and Olson, E. N. (1997) *Dev. Biol.* **187,** 311–321
46. Kim, S., Ip, H. S., Lu, M. M., Clendenin, C., and Parmacek, M. S. (1997) *Mol. Cell. Biol.* **17,** 2266–2278
47. Belaguli, N. S., Zhou, W., Trinh, T. H., Majesky, M. W., and Schwartz, R. J. (1999) *Mol. Cell. Biol.* **19,** 4582–4591
48. Kovacs, A. M., and Zimmer, W. E. (1998) *Gene Expr.* **7,** 115–129
49. Sawtell, N. M., and Lessard, J. L. (1989) *J. Cell Biol.* **109,** 2929–2937